

Spin polarization control by electric field gradients

Dan Csontos* and Sergio E. Ulloa

Department of Physics and Astronomy, and Nanoscale and Quantum
Phenomena Institute, Ohio University, Athens, Ohio 45701-2979

We predict that, in addition to the magnitude and sign of electric fields, the propagation of spin polarized carriers can be dramatically affected by *electric field gradients*. In particular, we show that spin polarization injection across semiconductor interfaces can be strongly suppressed or enhanced due to built-in, inhomogeneous electric fields. Furthermore, we show that the spin density *imbalance* and *polarization*, although used interchangeably in the literature, display diametrically different behavior in charge inhomogeneous systems. A generalized drift-diffusion equation that describes our findings is derived and verified by numerical calculations using the Boltzmann transport equation.

PACS numbers: 72.25.Dc, 72.25.Hg, 72.25.Rb, 72.25.Mk

Following the original Datta-Das proposal for a spin transistor,¹ and the emergence of the field of spintronics, there has been persistent and growing interest in spin injection and spin polarized transport in semiconductors. One great concern is how to efficiently inject spin-polarized electrons into a nonmagnetic semiconductor (NMS). While spin-polarization is easily achieved in ferromagnetic metals (FMs), injection of spin-polarized carriers into a NMS has proved difficult due to the “conductivity mismatch problem”.² A solution to this problem, originally proposed by Rashba³ and further analyzed by others,^{4,5,6} is to introduce a spin-selective tunneling barrier at the FM-NMS interface. An alternative interesting approach is based on the use of diluted magnetic semiconductors (DMSs)⁷ which enable the realization of all-semiconductor spintronic devices. Spin injection in DMS-NMS based structures has been demonstrated in several systems, such as vertical,⁸ lateral,^{9,10} and Zener/Esaki tunneling diode^{11,12,13} structures.

However, controlled electrical spin injection with high efficiency has been elusive. Furthermore, it has been shown experimentally that spin-polarized transport and injection is very sensitive to an applied bias,^{10,12,13,14,16} as well as different structural parameters such as doping concentrations¹⁴ and layer thicknesses.¹³ Thus, electric fields, although clearly influencing the charge degree of freedom, seem to also indirectly play a major role in spin-polarized transport. Recently, the electric-field dependence of spin-polarized transport in a charge homogeneous system was theoretically predicted.¹⁵

The role of inhomogeneous charge distributions and electric fields remains, however, unclear. Nevertheless, in experiments and realistic systems and devices, inhomogeneous electric fields are ubiquitous, whether introduced by design, or by intentional or unintentional small doping or material variations, which in particular is true on the submicron and nanometer scale. These considerations pose the fundamental question: *To what extent do inhomogeneous charge distributions and electric fields affect the spin degree of freedom, in particular around interfaces?*

In this letter, we show that, in addition to the magnitude and sign of electric fields,¹⁵ the propagation of spin

polarized carriers can be *dramatically* affected by *electric field gradients*, and that even weak inhomogeneities can significantly influence the spin polarization decay length. In particular, we show that spin-polarization injection across a DMS-NMS interface can be strongly suppressed or enhanced by electric field gradients due to built-in, inhomogeneous electric fields. Furthermore, we show that the spin density *imbalance* and *polarization*, although used interchangeably in the literature, display diametrically different behavior in charge inhomogeneous systems. A generalized drift-diffusion equation which is able to describe nonequilibrium spin density propagation in the presence of inhomogeneous electric fields is derived and verified with numerical calculations using the Boltzmann transport equation (BTE).

In order to fully understand spin transport properties in semiconductor structures, and in particular the influence of interfaces and inhomogeneous electric fields, one needs to take into account nonequilibrium transport processes for *both* the *charge* and *spin* degrees of freedom in a self-consistent way. In our approach, the transport of spin-polarized electrons is described by two BTE equations according to

$$-\frac{e}{m^*}\mathbf{E}\cdot\nabla_{\mathbf{v}}f_{\uparrow(\downarrow)}+\mathbf{v}\cdot\nabla_{\mathbf{r}}f_{\uparrow(\downarrow)}=-\frac{f_{\uparrow(\downarrow)}-f_{\uparrow(\downarrow)}^0}{\tau_m}-\frac{f_{\uparrow(\downarrow)}-f_{\downarrow(\uparrow)}}{\tau_{\uparrow\downarrow(\downarrow\uparrow)}}, \quad (1)$$

where \mathbf{E} is an inhomogeneous electric field, $f_{\uparrow(\downarrow)}$ is the electron distribution for the spin-up (down) electrons, τ_m is the momentum relaxation time, and $1/\tau_{\uparrow\downarrow}$ ($1/\tau_{\downarrow\uparrow}$) is the rate at which spin-up (spin-down) electrons scatter to spin-down (spin-up) electrons. The first term on the right-hand side of eq. (1) describes the relaxation of each nonequilibrium spin distribution to a local equilibrium (spin-dependent) electron distribution function, $f_{\uparrow(\downarrow)}^0$, which we choose as non-degenerate $f_{\uparrow(\downarrow)}^0 = n_{\uparrow(\downarrow)}\sqrt{\frac{m^*}{2\pi k_B T}}\exp(-m\mathbf{v}^2/2k_B T)$, where T is the lattice temperature. The last term in eq. (1) describes the relaxation of the spin polarization. From the distribution function $f_{\uparrow(\downarrow)}$ we calculate the local spin density according to $n_{\uparrow(\downarrow)} = \int f_{\uparrow(\downarrow)}d\mathbf{v}$ and define two quantities, the spin density *imbalance*, $\delta_{\uparrow\downarrow} = n_{\uparrow} - n_{\downarrow}$, where

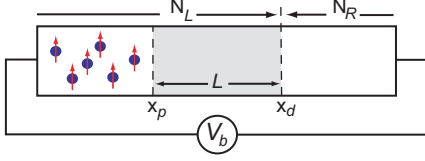


FIG. 1: (color online) Schematics of the model structure we consider. Full spin polarization, $P_n = 1$ is assumed for $x < x_p$.

n_\uparrow and n_\downarrow are the densities of spin-up and spin-down polarized electrons, and the spin density polarization, $P_n = (n_\uparrow - n_\downarrow)/(n_\uparrow + n_\downarrow) = \delta_{\uparrow\downarrow}/n$, where $n = n_\uparrow + n_\downarrow$ is the total charge density.

Charge interaction and inhomogeneous electric fields are taken into account by solving the Poisson equation

$$\nabla \cdot \mathbf{E} = e \frac{N_D - n_\uparrow - n_\downarrow}{\varepsilon \varepsilon_0}, \quad (2)$$

where ε is the dielectric constant and N_D is the donor concentration profile. The nonlinear, coupled equations (1,2) need to be solved self-consistently for a given applied bias voltage, doping concentration profile, nonequilibrium spin distributions, and relaxation times. Our theoretical model thus goes beyond drift-diffusion, and is capable of describing charge and spin transport through strongly inhomogeneous (with respect to spin and charge densities) semiconductor systems, as well as nonequilibrium effects. We assume in the following that an electric field is applied along the x direction and consider the corresponding one-dimensional transport problem. Details of the numerical procedure for a similar problem are given in Ref. 18.

The model structure we study is described in Fig. 1. As seen in the figure, the system is inhomogeneous with respect to both charge and spin degrees of freedom. Spin-polarized electrons, with $P_n = 1$, are injected from a DMS-like portion defined for $x < x_p$. The spin-polarized electrons subsequently relax due to spin-flip scattering for $x > x_p$, at the rate $1/\tau_{sf}$ (where $\tau_{\downarrow\downarrow} = \tau_{\downarrow\uparrow} = 2\tau_{sf}$), to the asymptotic unpolarized value $P_n = 0$ for $x \gg x_p$. The doping concentration is defined as $N_D = N_L$ and $N_D = N_R$ for $x < x_d$ and $x \geq x_d$, respectively. Thus, in the central region of length L , the electron spin and charge density distributions can be strongly inhomogeneous. The following material and system parameters have been used in our study: $T = 300$ K, $m^* = 0.067m_0$, $\tau_m = 0.1$ ps (typical for GaAs at room temperature), $\tau_{sf} = 1$ ns, $N_L = 10^{21} \text{ m}^{-3}$, $V_b = -0.3$ V.

In Fig. 2 we study the propagation of spin-polarized electrons across two spin- and charge-inhomogeneous interfaces, separated by $L = 0.2 \mu\text{m}$ (grey mid-region), as a function of different doping concentrations N_R . In Fig. 2(a) we show the spin density imbalance, $\delta_{\uparrow\downarrow} = n_\uparrow - n_\downarrow$ (solid lines), and the total charge density, n (dashed

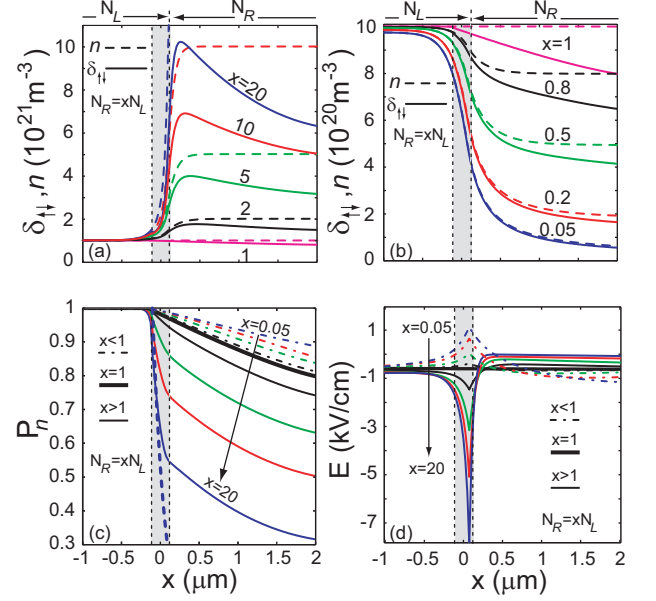


FIG. 2: (color online) Spin density imbalance $\delta_{\uparrow\downarrow}$ for $N_R \geq N_L$ (a) and $N_R \leq N_L$ (b), spin density polarization P_n (c), and electric field distribution (d) for a spin and charge inhomogeneous structure as depicted in Fig. 1, as a function of doping concentration, $N_R = xN_L$, $0.05 < x < 20$. The structure parameters are $N_L = 10^{21} \text{ m}^{-3}$, $L = 0.2 \mu\text{m}$, $\tau_{sf} = 0.5$ ns, $\tau_m = 0.1$ ps, $V_b = -0.3$ V.

lines), for $N_R = xN_L$, where $1 \leq x \leq 20$. The lowest solid and dashed curves correspond to a charge homogeneous sample, $N_R = N_L$, in which the field is accordingly constant, as shown by the thick, solid line in Fig. 2(d). In contrast to the constant total charge density, n , for the charge homogeneous case, the spin density imbalance, $\delta_{\uparrow\downarrow}$, decreases monotonically for $x > x_p$, which coincides with the onset of the spin flip scattering rate $1/\tau_{sf}$. The decay is exponential and can be understood in terms of the drift-diffusion description derived by Yu and Flatté:¹⁵ The spin density imbalance decay can be described by $\delta_{\uparrow\downarrow} \sim \exp[-x/L_{d(u)}]$ where

$$L_{d(u)} = \left\{ -(+) \frac{|eE|}{2k_B T} + \sqrt{\left(\frac{eE}{2k_B T} \right)^2 + \frac{1}{L_s^2}} \right\}^{-1}, \quad (3)$$

and where, $L_{d(u)}$ are electric-field dependent spin diffusion lengths, describing spin propagation antiparallel (parallel) to the electric field. In eq. (3) $L_s = \sqrt{D\tau_{sf}}$ is the intrinsic spin-diffusion length in the absence of an electric field and $D = k_B T \tau_m / m^*$, as obtained from the Einstein relation. From eq. (3) it follows that the spin-diffusion length is *enhanced* in the direction anti-parallel to an applied electric field and *suppressed* in the direction parallel to the field.¹⁵ Our numerical results agree with these considerations for the homogeneous system.

For inhomogeneously doped structures, $\delta_{\uparrow\downarrow}$ has a more complicated behavior, increasing with N_R , in contrast to the homogeneous case with $N_R = N_L$. Moreover, at the interface between the two regions with different doping concentrations, defined at x_d , a sharp increase of $\delta_{\uparrow\downarrow}$ is observed, displaying a peak-like structure for systems with larger N_R .¹⁷ As we will discuss below, the built-in electric fields result in this strong enhancement of the spin density imbalance.

For $N_R < N_L$, when electrons are injected from a high to a low doping region, the situation is reversed. In Fig. 2(b), the dashed and solid lines correspond to n and $\delta_{\uparrow\downarrow}$, calculated for different values of $N_R = xN_L$, where $1 \geq x \geq 0.05$. For decreasing N_R , $\delta_{\uparrow\downarrow}$ (and naturally n) decreases as well.

The observed increase (decrease) of $\delta_{\uparrow\downarrow}$ with increasing (decreasing) N_R can be understood in terms of the large difference between the intrinsic spin relaxation length, L_s , and the Debye screening length, L_{DB} . The screening length is typically much shorter than the intrinsic spin relaxation length. For example, for the range of doping concentrations considered here, we find $0.03 < L_{DB} < 0.6 \mu\text{m}$, whereas $L_s \approx 1.8 \mu\text{m}$. The spin density imbalance can be written in terms of $\delta_{\uparrow\downarrow} = n - 2n_{\downarrow}$. Since $L_s \gg L_{DB}$, the total charge density, n , will increase (decrease) faster than n_{\downarrow} with increasing (decreasing) N_R . Hence, the spatial dependence of n will dominate $\delta_{\uparrow\downarrow}$ within a screening length of the doping interface. This is clearly seen by comparison between $\delta_{\uparrow\downarrow}$ (solid lines) and n (dashed lines) in Figs. 2(a,b).

Deep into the right-hand side doping region, for $x \gg x_d$, $\delta_{\uparrow\downarrow}$ decreases monotonically away from the doping interface, due to the fact that the total charge density n is approximately constant beyond the screening length, and the spin-flip scattering drives the nonequilibrium spin density distribution toward equilibrium, $\delta_{\uparrow\downarrow} = 0$. Furthermore, $\delta_{\uparrow\downarrow}$ has a shorter decay length with increasing N_R . This is consistent with the predictions of eq. (3) since the electric field in that region decreases with an increase of N_R [see Fig. 2(d) for the electric field profiles].

The description provided by eq. (3), however, fails to describe the magnitude, as well as the spatial dependence of $\delta_{\uparrow\downarrow}$ around the doping interface. The discrepancy is particularly well illustrated by the spin density *polarization*, P_n , shown in Fig. 2(c). Notice that P_n is *strikingly different* from $\delta_{\uparrow\downarrow}$, and displays a *diametrically opposite dependence on position* for different values of N_R . In the region $x_p < x < x_d$, the spin density polarization corresponding to $N_R > N_L$ drops sharply below the value of P_n corresponding to the charge homogeneous case $N_L = N_R$. For $N_R < N_L$ on the other hand, the spin density polarization is higher than in the corresponding homogeneous case. In general, an increase (decrease) in N_R results in a decrease (increase) of P_n . This is in contradiction with eq. (3), from which it follows that an increase (decrease) in N_R should render an increase (decrease) in P_n due to the fact that a corre-

sponding increase (decrease) in the electric field occurs around the interface between the two regions with different doping concentrations [see Fig. 2(d)]. For example, for $N_R = 2 \cdot 10^{22} \text{ m}^{-3}$, the built-in electric field has the largest negative value [Fig. 2(d)] and should thus, according to eq. (3), result in the highest spin density polarization, in contrast to our results in which P_n in fact attains its lowest values.

The origin of the complex and diametrically different spatial behavior of P_n and $\delta_{\uparrow\downarrow}$, is due to the deviation from local charge neutrality around the interface, and the corresponding inhomogeneous electric fields. Previous works have mainly focused on the charge homogeneous case.^{4,5,15,19} This is a natural assumption since the screening length is expected to be much shorter than the spin relaxation length, leading one to assume quasi-local charge neutrality. However, as we will show below, even quasi-local deviations from charge neutrality can have a very strong impact on the spin polarization and dramatically suppress the spin injection efficiency.

By relaxing the assumption of local charge neutrality, and using the same drift-diffusion, steady-state approach as in Refs. 15 we find that $\delta_{\uparrow\downarrow}$ satisfies a drift-diffusion equation:

$$\nabla^2 \delta_{\uparrow\downarrow} + \frac{e}{k_B T} \mathbf{E} \cdot \nabla \delta_{\uparrow\downarrow} + \frac{e}{k_B T} \delta_{\uparrow\downarrow} \nabla \cdot \mathbf{E} - \frac{1}{L_s^2} \delta_{\uparrow\downarrow} = 0. \quad (4)$$

Compared to the equation derived before,¹⁵ eq. (4) contains an additional term, proportional to the *gradient* of the electric field, $\nabla \mathbf{E}$. One can define spin imbalance decay lengths, similar to those defined in eq. (3), according to:

$$L'_{d(u)} = \left\{ -(+) \frac{|eE|}{2k_B T} + \sqrt{\left(\frac{eE}{2k_B T} \right)^2 + \frac{1}{L_s^2} - \frac{e \nabla E}{k_B T}} \right\}^{-1}. \quad (5)$$

Notice $L'_{d(u)}$ are defined only “locally”, valid over a region in which ∇E is nearly constant, so that one can define the exponential dependence of $\delta_{\uparrow\downarrow}$. The drift-diffusion lengths depend strongly on the *gradient* of the electric field; Consequently, the spin density imbalance and polarization decay lengths are enhanced or suppressed based not only on the sign of the electric field alone.¹⁵ On the contrary, depending on the profile of the electric field, the gradient term in eq. (5) can either enhance or suppress the spin-polarization propagation significantly, as seen explicitly in our calculated results in Fig. 2(a-c).

To illustrate the dramatic impact of the field gradient term on the spin polarization diffusion, we calculate $L'_{d(u)}$ for the central region of the structure, $x_p < x < x_d$. Using a linear approximation of the electric field within the channel region for the structure with $N_R = 2 \cdot 10^{22} \text{ m}^{-3}$ [blue solid line in Fig. 2(c)], the intrinsic spin-diffusion length $L_s \approx 1.8 \mu\text{m}$, and an electric field value taken at

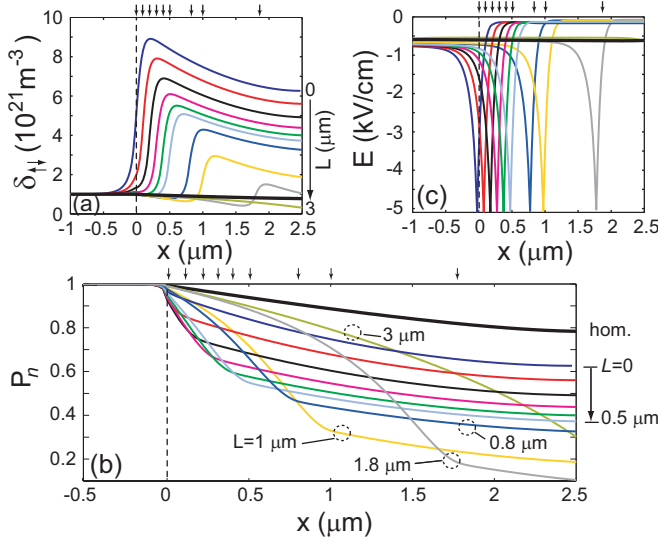


FIG. 3: (color online) Spin density imbalance $\delta_{\uparrow\downarrow}$ (a), spin density polarization P_n (b), and electric field distribution (c) for a spin and charge inhomogeneous structure as depicted in Fig. 1, for different channel lengths, $L = 0, 0.1, 0.2, 0.3, 0.4, 0.5, 0.8, 1.0, 1.8, 3.0 \mu\text{m}$. Curves are offset such that $x_p = 0$ in all cases. Parameters are $N_L = 10^{21} \text{ m}^{-3}$, $N_R = 10^{22} \text{ m}^{-3}$, $\tau_{sf} = 1 \text{ ns}$, $\tau_m = 0.1 \text{ ps}$, $V_b = -0.3 \text{ V}$. Arrows indicate the position at x_d .

mid-channel, $E = -2.9 \text{ kV/cm}$, eq. (5) yields $L'_d \approx 0.16 \mu\text{m}$ and $L'_u \approx 0.06 \mu\text{m}$. In comparison, an evaluation of eq. (3) using the same value of the electric field, yields $L_d \approx 36 \mu\text{m}$, $L_u \approx 0.09 \mu\text{m}$. Hence, the electric field gradient in this case decreases the “local” (around the interface) spin diffusion length, along the direction of (charge) transport, by two orders of magnitude! *The injected spin density polarization is thus destroyed by the inhomogeneous electric field at the doping interface.*

To verify the validity of eq. (5), we compare $\delta_{\uparrow\downarrow} \propto \exp[-(x - x_p)/L'_d]$, using $L'_d = 0.16 \mu\text{m}$ as before, with the results (for P_n) from our Boltzmann-Poisson numerical calculation, within $x_p < x < x_d$. The results, plotted in Fig. 2(c) (thick dashed, blue line, for the highest N_R value), are found to agree very well with the numerically calculated values.

Reversing the sign of the electric field gradient, the spin density polarization P_n is in fact *enhanced* in comparison to the homogeneous case. This is illustrated by the dashed-dotted curves in Fig. 2(c), which correspond to $N_R < N_L$. Since the electric field gradients are not as large as for the previously studied case [see Fig. 2(d)], the corresponding increase in P_n is more modest.

We note that spin accumulation at the interface between regions with different doping concentrations, such as seen in Fig. 2(a), has been previously discussed by Pershin and Privman.¹⁷ They argued that injecting spin-polarized electrons across a low-to-high doping concentration interface yields a significant enhancement of the

spin polarization. However, the increase is seen only for $\delta_{\uparrow\downarrow}$, i.e., the spin density *imbalance*, which the authors considered in their work. This is, however, only due to the overall total charge density increase as discussed above. The actual spin density *polarization*, P_n , on the other hand, is dramatically *suppressed*, as clearly shown by our study, due to the built-in electric field at the interface and more importantly due to the negative electric field gradients. Moreover, we find that P_n can be enhanced for spin-polarized electron injection across a high-to-low doping concentration interface, due to the positive electric field gradients [see dashed-dotted lines in Fig. 2(c)].

We further clarify the effects of electric field gradients on the relaxation of nonequilibrium spin distributions. Figure 3 shows the results for $\delta_{\uparrow\downarrow}$ (a), P_n (b), and $E(x)$ (c) calculated for $N_R = 1 \cdot 10^{22} \text{ m}^{-3}$ and different channel lengths, $0 < L < 3 \mu\text{m}$. We have offset all curves in space such that x_p , i.e., the DMS/NMS interface, coincides. For $L = 0$, $\delta_{\uparrow\downarrow}$ shows a sharp increase around the doping interface, followed by a monotonic, exponential decrease, whereas the spin density polarization, P_n , shows an exponential decrease only, with decay length similar to $\delta_{\uparrow\downarrow}$, but with values below the corresponding values for the homogeneous system (thick solid line). This is in agreement with our previous discussion and agrees with the fact that the electric field [see Fig. 3(c)] in the right-hand side region is significantly lower than for the homogeneous case [thick solid line in Fig. 3(c)].

For increasing channel lengths the spin imbalance decreases significantly. In particular, $\delta_{\uparrow\downarrow}$ for the inhomogeneous structure is *smaller* than the corresponding homogeneous one (thick solid line) for $x < x_d$ and a dip-like feature is formed for large L prior to the interface between the two doping regions, where $\delta_{\uparrow\downarrow}$ is seen to increase and reach a peak. Interestingly, this also occurs for $x < x_d - L_{DB}$ for the structures with $L \gg L_{DB}$, i.e., in a region with very small electric field gradients [see Fig. 3(c)]. This illustrates the fact that, although the electric field gradients in this region are very small [virtually unobservable on the scale shown in Fig. 3(c)], they are large enough to yield significant influence on the spin density imbalance. In the spin density polarization, P_n , the inhomogeneous electric fields manifest as nonexponential spatial dependence, which further accentuates the importance of electric field gradients in the propagation of spin-polarized carriers.

Our results suggest that spin polarized injection, transport and detection can be dramatically influenced by the details of the electrostatics and that tailoring of the band-structure may enable the design of semiconductor spintronics.

This work was supported by the Indiana 21st Century Research and Technology Fund. Numerical calculations were performed using the facilities at the Center for Computational Nanoscience at Ball State University.

-
- * Electronic address: csontos@phy.ohiou.edu
- ¹ S. Datta, and B. Das, Appl. Phys. Lett. **56**, 665 (1990).
 - ² G. Schmidt *et al.*, Phys. Rev. B **62**, R4790 (2000).
 - ³ E. I. Rashba, Phys. Rev. B **62**, R16 267 (2000).
 - ⁴ S. Agrawal *et al.*, Phys. Rev. B **72**, 075352 (2005).
 - ⁵ V. V. Osipov, and A. M. Bratkovsky, Phys. Rev. B **72**, 115322 (2005).
 - ⁶ A. Fert, and H. Jaffrès, Phys. Rev. B **64**, 184420 (2001).
 - ⁷ H. Munekata *et al.*, Phys. Rev. Lett. **63**, 1849 (1989); H. Ohno, Science **281**, 951 (1998), and references therein.
 - ⁸ R. Fiederling *et al.*, Nature **402**, 787 (1999); Y. Ohno *et al.*, Nature **402**, 790 (1999).
 - ⁹ G. Schmidt *et al.*, Phys. Rev. Lett. **87**, 227203 (2001).
 - ¹⁰ G. Schmidt *et al.*, Phys. Rev. Lett. **92**, 226602 (2004).
 - ¹¹ E. Johnston-Halperin *et al.*, Phys. Rev. B **65**, 041306(R) (2002).
 - ¹² P. Van Dorpe *et al.*, Appl. Phys. Lett. **84**, 3495 (2004).
 - ¹³ M. Kohda *et al.*, condmat/0508371.
 - ¹⁴ C. Adelmann *et al.*, J. Vac. Sci. Technol. **23**, 1747 (2005).
 - ¹⁵ Z. G. Yu, and M. E. Flatté, Phys. Rev. B **66**, 201202(R) 2002; Z. G. Yu, and M. E. Flatté, *ibid.* **66**, 235302 (2002).
 - ¹⁶ S. A. Crooker, and D. L. Smith, Phys. Rev. Lett. **94**, 236601 (2005).
 - ¹⁷ Y. V. Pershin, and V. Privman, Phys. Rev. Lett. **90**, 256602 (2003).
 - ¹⁸ D. Csontos, and S. E. Ulloa, condmat/0507427.
 - ¹⁹ H. Dery *et al.*, Phys. Rev. B **73**, 041306(R) (2006).